Tetrahedron Letters xxx (2018) xxx–xxx

Contents lists available at ScienceDirect

Tetrahedron Letters

journal homepage: www.elsevier.com/locate/tetlet

A red emissive donor-acceptor fluorophore as protein sensor: Synthesis, characterization and binding study

Rajib Choudhury *, Hope E. Parker, Kassandra M. Cendejas, Kalie L. Mendenhall

Department of Physical Sciences, Arkansas Tech University, Russellville, AR 72801, United States

ARTICLE INFO

Article history:
Received 15 May 2018
Revised 27 June 2018
Accepted 28 June 2018
Available online xxxx

Keywords:
Donor-acceptor fluorophores
Solvatochromism
Human serum albumin
Intramolecular charge transfer

ABSTRACT

The rational design of environmentally sensitive small molecule fluorophores with superior photophysical properties is critical for fluorimetry based biosensing. Herein, we have developed a new donor-acceptor fluorophore for quantitative detection of Human Serum Albumin (HSA) in aqueous samples. The fluorophore was easily prepared by Knoevenagel condensation, and showed excellent photophysical properties and positive solvatochromism. The design of the fluorophore was based on a nitrogen donor–π-conjugation–nitrile acceptors (D–π–A) to preserve efficient intramolecular charge transfer and long-wavelength emission. The fluorophore showed remarkable "turn-on" fluorescence in presence of HSA, which led to quantitative determination of the protein in aqueous buffer samples. Structure and electronic properties of the fluorophore played important roles on the superior HSA sensing ability. The findings indicate that minor changes in design strategy can be advantageous while developing long-wavelength (far red or near infrared) emitting fluorophores for biosensing and bioimaging.

Introduction

Fluorimetric detection of biological molecules is of great importance in the field of biology and medicine [1–3]. Among many analytical techniques available fluorescence method stands out due to its high sensitivity and selectivity. Fluorometer is easy to operate, quick, and relatively inexpensive [3]. But, a suitable fluorophore is always required for quantitative detection of a target molecule in samples. Several promising new fluorophores have been described in literature, although selectivity and sensitivity could be improved [4–6].

In this context, environment sensitive fluorophores are very useful as "turn-on" fluorescent probes [7–12]. Such fluorophores can be inserted within a protein's cavity by simple solution mixing. However, optimum stereoelectronic and steric properties will play major roles in this process. Upon complexation, restricted movements and specific interactions within the protein's microenvironment alter photophysical properties of the fluorophore, which result in distinguishable and measurable spectral signals [3]. Moreover, a greater sensitivity is obtained when studies are performed in the near-infrared region (NIR, 650–900 nm), as scattering of light and interference from other biological molecules in samples remain minimal [13–19].

Herein, we have designed and reported a new far red emissive donor-acceptor (D–π–A) fluorophore (Scheme 1). An efficient intramolecular charge transfer (ICT) between the highly positive mesomeric donor (-NMe_2) and the powerful electron acceptor (tricyanofuran, TCF) has enabled quantitative detection of a protein, Human serum Albumin (HSA), in the red region (~650 nm) of the spectrum [20]. The fluorescence signal was intensified upon inclusion of the fluorophore within the protein's pocket; a tighter supramolecular complexation impeded non-radiative decay by restricting rotational degrees of freedom and hence increased the quantum yield of the fluorophore.

HSA is the most abundant protein in blood plasma. It is an important biomarker that can indicate a wide range of health conditions such as renal disease, coronary artery disease, stroke, and liver or kidney failure, especially for those with diabetes [21–25]. Therefore, a simple and cost-effective fluorimetric method for quantitative detection of HSA in samples is highly desirable.

Here, a small molecule D–π–A fluorophore with a polar $-CH_2CH_2OH$ group has enabled milligram level detection of HSA by fluorescence spectroscopy in aqueous buffer samples. The fluorophore binds selectively with HSA driven by hydrophobic and van der Waals type interactions. Lack of any aggregate formation in aqueous solution has resulted spontaneous supramolecular complex formation with HSA. In physiological buffer condition, detection limit for HSA was 30 nano-molar, which may be useful in point-of-care medical diagnosis in near future.

* Corresponding author.
E-mail address: rchoudhury@atu.edu (R. Choudhury).

https://doi.org/10.1016/j.tetlet.2018.06.064
0040-4039/

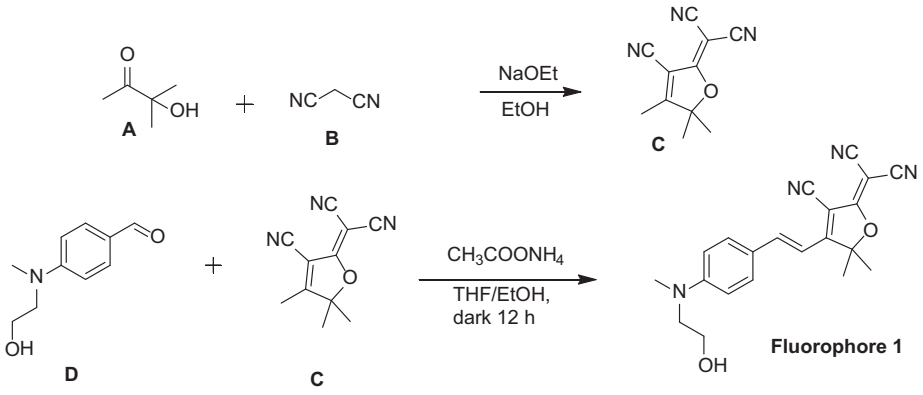

Scheme 1. Synthesis route for fluorophore **1**.

Results and discussion

Fluorophore **1** was synthesized following a literature report as shown in Scheme 1 [26]. In the first step 3-hydroxy-3-methylbutan-2-one (**A**) was coupled to malononitrile (**B**) to yield 2-(3-cyano-4,5,5-trimethylfuran-2(5H)-ylidene)malononitrile (**C**) as off-white powder (yield 48.4%). Knoevenagel condensation between **C** and 4-((2-hydroxyethyl)(methyl)amino)benzaldehyde (**D**) provided target fluorophore **1** in 44.5% yield. Detailed synthesis procedure and characterization results (FTIR, ^{1}H and ^{13}C NMR, ESI data, and elemental analysis) are provided in the Supporting information. The selectivity of Knoevenagel condensation to all-trans isomer was very high within the limits of NMR detection (Figs. S1 & S2). Presence of vinylic protons was confirmed from NMR coupling constant ($J \approx 16$ Hz) and the purity of the compound was confirmed by mass and elemental analysis.

Fluorophore **1** was highly soluble in polar aprotic solvents such as, acetonitrile, dichloromethane, dimethylsulfoxide (DMSO), dimethylformamide (DMF) as well as in polar protic solvents such as, ethanol, methanol, and isopropanol. It had minimal solubility in water at physiological pH.

Solution of fluorophore **1** exhibited different colors in different solvents (Fig. S3) [27,28]. For instance, pink in toluene, ethyl acetate, and acetone; blue in acetonitrile, DMF, and DMSO; purple in ethanol, methanol, and water. Fig. 1a shows absorption spectra of **1** ([**1**] = 1.0×10^{-5} M) in ten different solvents including water at pH 7.4 (λ_{max} = 587 nm; ε = 40,000 M^{-1} cm^{-1}). Absorption maxima (λ_{max}) in nonpolar solvents such as toluene and ethyl acetate were at 562 nm and 565 nm, respectively. With increased polarity of the solvents λ_{max} bathochromically shifted, indicating positive solvatochromism (Table S1). The longest absorption maxima recorded was in DMSO (λ_{max} = 595 nm). All these bands most likely arise from n–π^* electronic transition with an intramolecular charge transfer (ICT) from donor –NMe_2 to acceptor TCF [27].

Emission of **1** was recorded concurrently in the same set of solvents. Fig. 1b shows broad emissions of **1** in ten different solvents, ranging from yellow (in toluene, λ_{max} = 614 nm) to NIR-I region (in DMSO, λ_{max} = 665 nm) of the spectrum. Bathochromic shift was observed as polarity of the solvents increased, confirming positive solvatochromism of **1** (Table S2) [8,27]. Excitation spectra were recorded simultaneously to confirm that no fluorescent impurities were present in solution. Nice overlap with absorption spectra ruled out the possibility of presence of any secondary fluorescent species.

To be suitable for application in biological samples, fluorophore **1** must ideally remain as monomer in water. Therefore, aggregate formation of **1** was examined in water by recording absorption spectra with varying concentrations (up to 2.0×10^{-5} M) and then calculating molar extinction coefficients (ε) at those concentrations. Identical ε values indicate that **1** primarily remains as monomer in aqueous solution. Therefore, the emission spectrum of **1** in water ([**1**] = 1.0×10^{-5} M; pH = 7.4; λ^{em}_{max} = 647 nm) was recorded and adopted as working concentrations for all the experiments, unless otherwise stated. Moreover, absorption and emission spectra remained unchanged in the pH range of 4.0–10.0, indicating good pH tolerance of fluorophore **1** for potential biological applications (Fig. S4).

Fluorescence of donor-π-acceptor fluorophores is highly environment sensitive [8,12]. Due to intramolecular charge transfer a

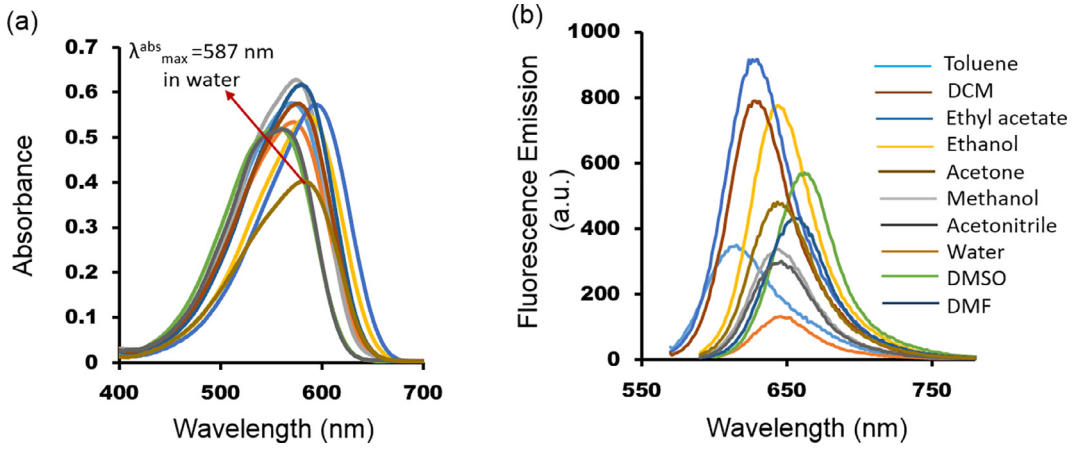

Fig. 1. (a) Absorption spectra of fluorophore **1** in various solvents. [**1**] = 1.0×10^{-5} M. Aqueous solution contains 1% DMSO. (b) Emission spectra of **1** in various solvents. [**1**] = 1.0×10^{-5} M. Aqueous solution contains 1% DMSO.

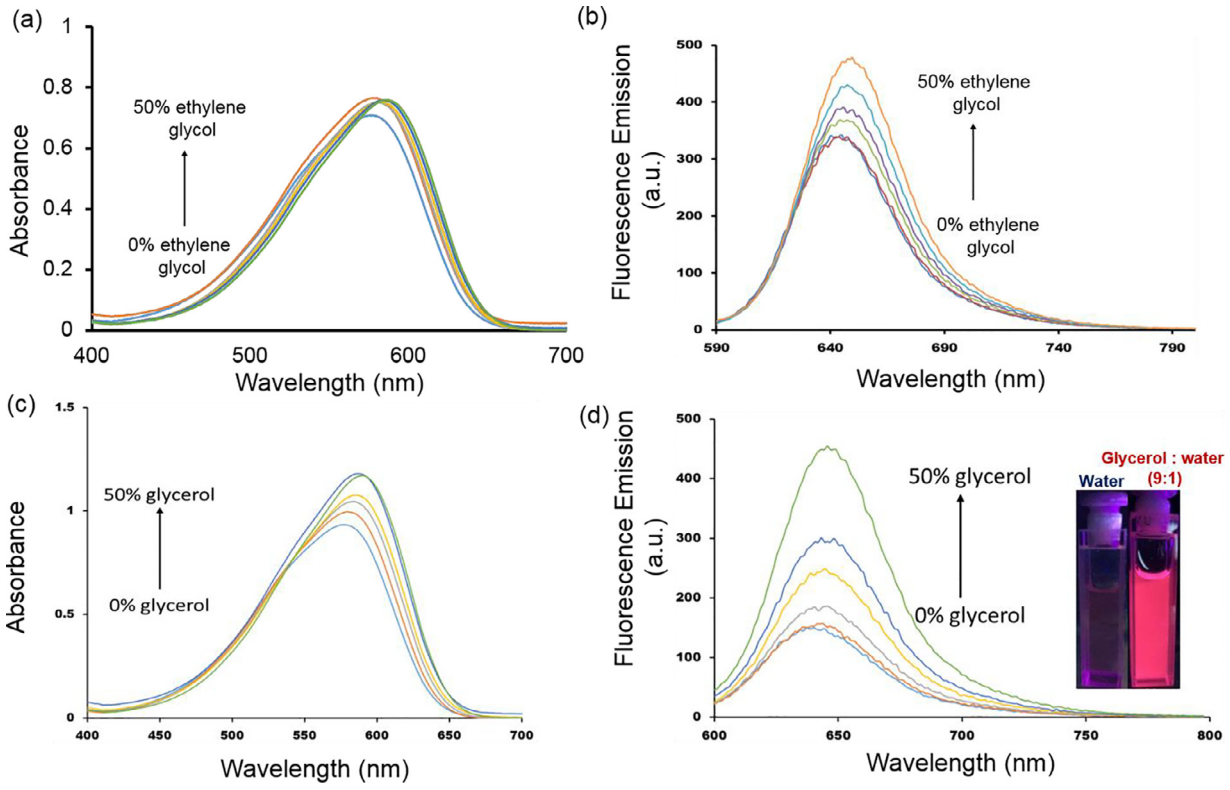

Fig. 2. (a) Absorption spectra of **1** with added ethylene glycol in methanol. (b) Emission spectra of **1** with added ethylene glycol in methanol. (c) Absorption spectra of **1** with added glycerol in methanol. (b) Emission spectra of **1** with added glycerol in methanol. [**1**] = 1.0×10^{-5} M; Inset: Appearance of bright red fluorescence emission in glycerol/water (9:1) mixture.

dipole moment is generated in the ground state, which becomes very large upon excitation of an electron in the excited state. Therefore, any excited state phenomenon including radiative decay energy and the concomitant quantum yield is very sensitive to the surrounding of the fluorophore, specifically to the polarity of the solvents [26]. Moreover, in hydrogen bonding solvents such as in water excited state energy can dissipate via other non-radiative decay channels [29,30]. Therefore, quantum yield of the D—π—A fluorophores in water is usually low. The quantum yield (Φ_F) of **1** was <0.01 in water with respect to the standard rhodamine B.

Quantum yield of ICT fluorophores comprising flexible or rotatable bonds is highly sensitive to the rigidity of the microenvironment. Usually, Φ_F increases as the viscosity of the medium increases due to suppression of the intramolecular twists of the rotatable bonds in the main π-conjugated backbone on the excited state manifold. Therefore, in a high viscous environment, loss of fluorescence energy via non-radiative pathway is suppressed, and hence a significant increase in quantum yield is observed [29]. Similar trends were observed for **1** in high viscous liquids such as ethylene glycol (35.7 cP at 25 °C) and glycerol (950 cP at 25 °C). Fig. 3 shows absorption and emission spectra of **1** in ethylene glycol/methanol and glycerol/methanol mixtures. Absorption maxima bathochromically shifted 4 nm and 10 nm in 1:1 ethylene glycol/methanol and glycerol/methanol mixture, respectively. Emission intensity significantly increased upon addition of ethylene glycol or glycerol in methanolic solution of **1**. Emission quantum yields in ethylene glycol/methanol (1:1) and glycerol/methanol (1:1) were 0.04 and 0.11, respectively. This confirms that the fluorescence of **1** is highly sensitive to the microenvironment and has the potential for biosensing applications, since emission signals can be intensified by restricting the movements and rotations of the fluorophore within the microenvironment of the biomolecules.

Next, we sought to exploit this property of the ICT fluorophores for quantitative detection of Human Serum Albumin (HSA) in physiological pH. In a solution of fluorophore **1** (phosphate buffer, pH 7.4), HSA was gradually added and absorption and emission spectra were recorded at room temperature. Absorption maxima of **1** shifted both bathochromically and hyperchromically as more HSA was added. Emission intensity increased as well with increasing amount of HSA (Fig. 3a). Quantum yield of **1** jumped to 0.34 from less than 0.01 in presence of 1% of HSA. All the changes in spectral characteristic indicate successful inclusion of **1** within the protein's cavity. To get a quantitative estimate of the extent of binding, association constant (K_a) was calculated using Benesi-Hildebrand relation [31]. As shown in Fig. 3b, plot of $1/(I - I_0)$ vs $1/[HSA]$ resulted a straight line, indicating 1:1 complexation between **1** and HSA. From the ratio of the slope and the intercept corresponding binding affinity ($K_a = 1.47 \times 10^5\ M^{-1}$) was calculated.

The high association constant and the corresponding large fluorescence enhancement suggests that in presence of **1** a very small amount of HSA detection would be possible in aqueous samples. To determine the detection limit, fluorescence titration of **1** with HSA was carried out by adding aliquots of HSA in a buffered solution of **1**. Fluorescence intensity was plotted as a function of concentration of HSA and detection limit was calculated from the IUPAC recommendation of 3σ/k equation (Fig. 3c) [32]. It was found to be 2 mg/L (2 ppm), which indicates that in presence of **1** minimum amount of HSA can be detected fluorimetrically is 2 mg per liter of sample. Moreover, fluorescence intensity of **1** at emission maxima showed an excellent correlation ($R^2 = 0.991$) to the amount of HSA over the range of 0.020 mg/L to 0.4 mg/L (Fig. 3c). This finding demonstrates that fluorophore **1** has potential for quantitative detection of HSA in human urine samples. In this aspect it is important to highlight that **1** has reached to the very low detection limit

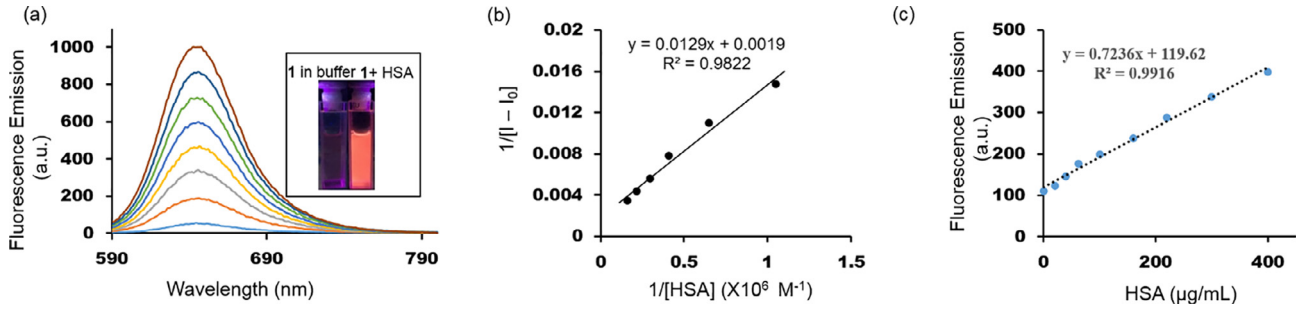

Fig. 3. (a) Effect of increasing amount of HSA on the fluorescence emission of **1**, [**1**] = 1.0×10^{-5} M. Inset: Appearance of red fluorescence upon addition of HSA, [HSA] = [**1**] = 6.65×10^{-7} M. (b) Benesi-Hildebrand plot of $1/[I - I_0]$ vs 1/[protein] (M^{-1}) for binding of **1** with HSA. (c) Linear relationship between emission maxima and HSA concentration. Detection limit 2 mg/L from 3σ/k; σ is standard deviation between blank measurements; k is slope between fluorescence intensity vs [HSA].

ranges reported by Das et al. (detection limit ≈ 6.5 nm) and Kumar et al. (detection limit = 11 nm), and it has shown lower detection limit than other fluorophore based reported HSA sensors (Cheng. et al., detection limit = 140 nM; Xu et al., detection limit = 140 nM; Ramezani et al., detection limit = 62 nM) [33–37].

The dramatic environment sensitivity of fluorophore **1** upon binding with HSA prompted us to investigate the location of the probable binding site(s) in the protein. HSA has three major domains (I, II, and III), which are divided into two subdomains (A and B). Small molecules, drugs, and fatty acids normally bind to site I (domain I and II) by hydrophobic interactions, whereas binding to site II (domain III) involves a combination of hydrophobic, hydrogen bonding, and electrostatic interactions [38,39]. Phenylbutazone, a site specific hydrophobic drug, binds into subdomain IIA ($K_a = 7.0 \times 10^5$ M^{-1}) with very high affinity [40,41]. In our study, addition of aliquots of phenylbutazone into a solution of **1**@HSA reduced the fluorescence intensity of **1**. Addition of excess drug resulted complete displacement of **1** from the protein cavity (Fig. S5). Moreover, in another set of titrations addition of equal molar amount of palmitic acid reduced the fluorescence intensity of **1** by half, indicating displacement of the fluorophore from HSA binding site (Fig. S6) [42–45]. Ibuprofen, a site III A specific binder did not displace **1** from the HSA (Fig. S7). Addition of even two hundred times of ibuprofen had no effect on the emission intensity of **1**, suggesting site I as the preferable binding location for **1**. Based on these displacement titration experiments, we tentatively attribute that fluorophore **1** binds to site I driven by both hydrophobic and van der Waals interactions.

To understand the influence of structure and property of a fluorophore on the binding and sensing of a protein in aqueous

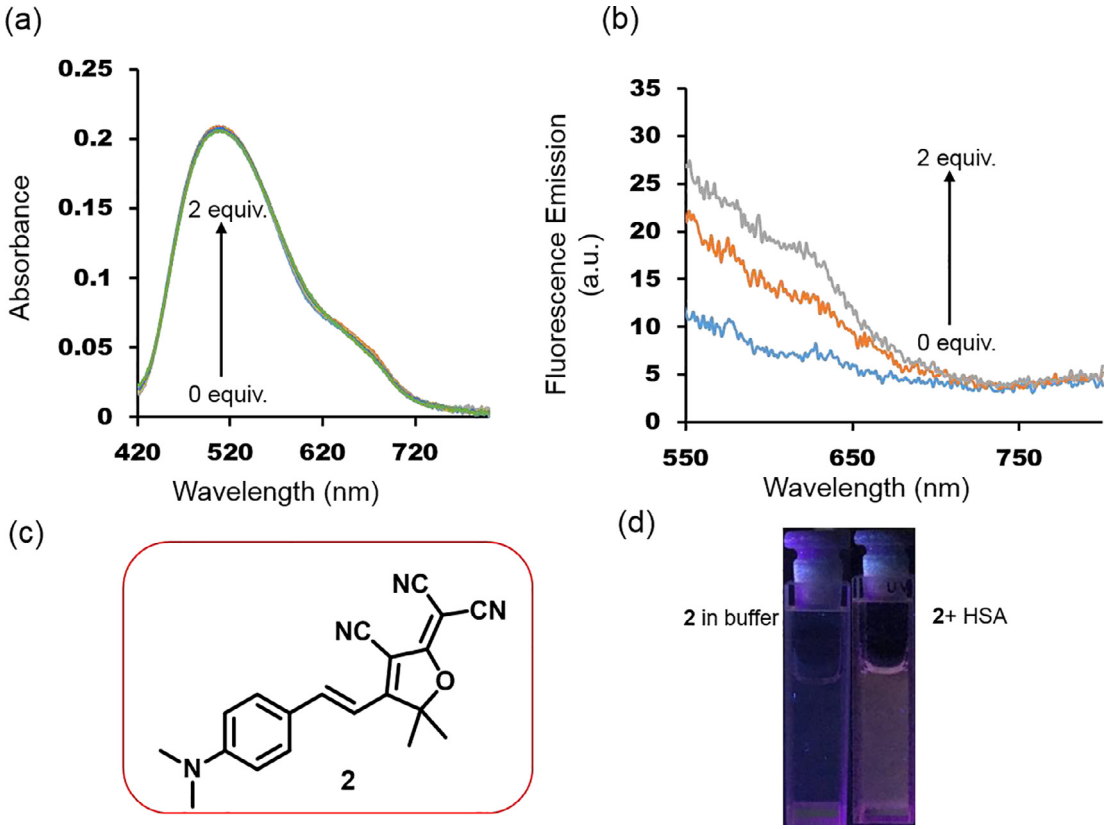

Fig. 4. (a) Effect of increasing amount of HSA, up to 2 equiv. on the absorption of **2**, [**2**] = 1.0×10^{-5} M. Five aliquots of HSA were added to reach 2 equivalent. Aqueous solution contains 1% DMSO. (b) Effect of increasing amount of HSA, up to 2 equiv. on the fluorescence emission of **2**, [**2**] = 1.0×10^{-5} M. Aqueous solution contains 1% DMSO. (c) Structure of fluorophore **2**. (d) Appearance of emission of **2** upon addition of HSA; [HSA] = [**2**] = 6.65×10^{-7} M.

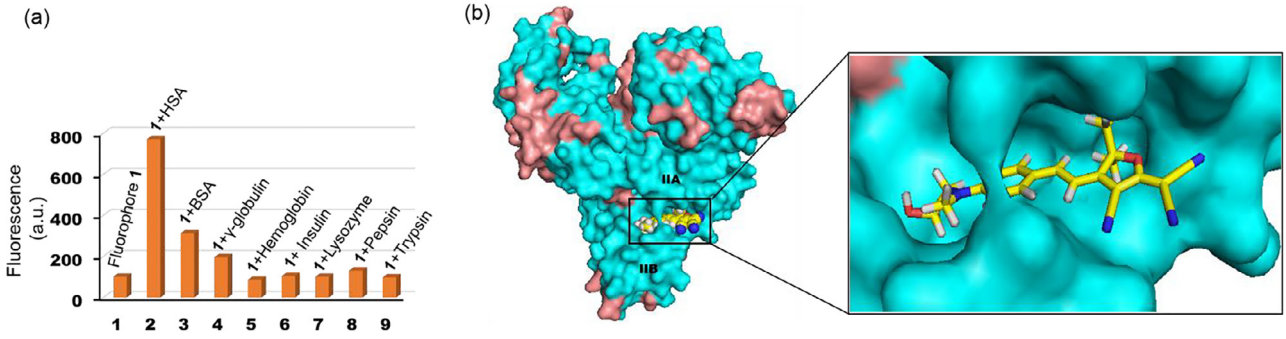

Fig. 5. (a) Fluorescence emission intensity of **1** in presence of various other proteins. (b) Lowest binding energy docking conformation of **1** within the HSA.

samples, a derivative of fluorophore **1** (**2**, λ_{em} = 650 nm in DMSO/phosphate buffer, 2:8, v/v) was prepared [46,47]. The only structural difference between **1** and **2** was that, in **2** the $-CH_2CH_2OH$ chain was replaced with a methyl group. Fluorophore **2** formed H-type aggregate in water (λ_{max} = 492 nm; Figs. 4a and S8), which was inferred from extreme broadening and blue shift of the spectrum in water. No emission was recorded in deionized water and phosphate buffer, though it was fluorescent in organic solvents. Addition of even excess HSA (up to 2 equivalents) did not result in any emission (Fig. 4). However, it formed complexes with HSA in 2:8 DMSO: buffer mixture, which was evident from intensified emission signals. Gradual addition of HSA enhanced the emission intensity along with the blue shift of the emission maxima (Fig. S9). The results demonstrate the importance of optimum structure and property of a fluorophore in sensing and detection of a biomolecule in aqueous samples.

To obtain the selective binding of **1** with HSA, fluorescence spectra were measured in presence of various other proteins (Fig. 5a). Addition of one equivalent of each protein to a buffered solution of **1** (10 μM) had negligible effect on the emission intensity. Only bovine serum albumin (BSA) increased the emission of **1** by 1.5-fold, indicating complexation of **1** with BSA to a marginal amount.

Furthermore, to obtain a visual perspective of the geometry of the stable conformation of **1** upon binding to HSA, molecular docking was carried out on AutoDock Vina program [48]. Total nine conformations of **1** were obtained from docking, ranked from lowest to highest binding energy (Table S3). Fig. 5b depicts the best binding structure (−8.3 kcal/mol) between **1** and HSA. It binds within the interface between subdomain IIA and IIB with high affinity (Fig. 5b). The negative and high binding energy suggests that the binding is spontaneous and energetically favorable process.

In summary, Benesi-Hildebrand plot suggests that **1** forms strong complex with HSA. Site specific displacement titrations and molecular docking studies indicate that **1** binds within the site I. The increased fluorescence of **1** upon binding with HSA resulted most likely due to the suppression of the twisted intramolecular charge transfer (TICT) state [49,50]. While within the protein's cavity, van der Waals interactions with the amino acids as well as narrow space rigidify the conformation of the fluorophore, suppressing the non-radiative decay.

The fluorescence intensity of **1** decreased and red shifted with increase in polarity of the solvents from ethyl acetate to dichloromethane to dimethyl sulfoxide, indicating existence of twisted intramolecular charge transfer in the system (Table S2) [49,50]. Moreover, strong viscosity dependence of the emission intensity suggests that TICT exists and it weakens the fluorescence of the compound through non-radiative decay [1,49] (Fig. 2). The fluorescence can be recovered upon strong non-covalent association with HSA.

Conclusions

We have designed, synthesized, and characterized a donor-acceptor (D-A) fluorophore which emits in the red region of the electromagnetic spectrum. Incorporation of a tailored nitrogen donor and a TCF acceptor in the D—π—A chain has resulted efficient ICT and improved photophysical properties in aqueous solution. Upon immobilization within HSA, the fluorophore exhibited very high emission quantum yield due to TICT suppression, which has enabled milligram level detection of the protein by steady state fluorescence spectroscopy.

This study illustrates the importance of suitable combination of donor and acceptor moieties while designing a "turn-on" fluorophore sensor for specific application. Our future efforts will include assessing the efficacy of the fluorophore for specific and quantitative detection of albumin in human urine samples and design of new fluorophores in the NIR-I window for superior performance in biological samples.

Acknowledgements

We acknowledge support from the undergraduate research office at Arkansas Tech University for financial support. We wish to thank Dr. Anindya Ghosh at UALR for collecting and providing the NMR and mass spectrometry results included in this publication.

Notes

The authors declare no competing financial interest.

A. Supplementary data

Supplementary data associated with this article can be found, in the online version, at https://doi.org/10.1016/j.tetlet.2018.06.064. These data include MOL files and InChiKeys of the most important compounds described in this article.

References

[1] H.-J. Guder, D. Heindl, H.-P. Josel, Overview of colorimetric, chemiluminometric, and fluorimetric detection systems, in: C. Kessler (Ed.), Nonradioactive Analysis of Biomolecules, Springer, Berlin, 2000, Ch 15.
[2] W. Rettig, B. Strehmel, S. Schrader, H. Seifert, Applied Fluorescence in Chemistry, Biology, and Medicine, Springer, Berlin, 2012, Ch 4-5.
[3] J.R. Lakowicz, in: J.R. Lakowicz (Ed.), Principles of Fluorescence Spectroscopy, Springer, New York, 2011.
[4] K. Rajasekhar, J.A. Chaithra, T. Govindaraju, Org. Biomol. Chem. 15 (2017) 1584–1588.
[5] M.M. McCallum, A.J. Pawlak, W.R. Shadrick, A. Simeonov, A. Jadhav, A. Yasgar, D.J. Maloney, L.A. Arnold, Anal. Bioanal. Chem. 406 (2014) 1867–1875.
[6] T.M.S. Goncalves, Chem. Rev. 109 (2009) 190–212.

[7] S.Y. Nishimura, S.J. Lord, L.O. Klein, K.A. Willets, M. He, Z. Lu, R.J. Twieg, W.E. Moerner, J. Phys. Chem. B 110 (2006) 8151–8157.
[8] S.J. Lord, Z. Lu, H. Wang, K.A. Willets, P. James Schuck, H.D. Lee, S.Y. Nishimura, R.J. Twieg, W.E. Moerner, J. Phys. Chem. A 111 (2007) 8934–8941.
[9] K.A. Willets, S.Y. Nishimura, P. James Schuck, R.J. Twieg, W.E. Moerner, Acc. Chem. Res. 38 (2005) 549–556.
[10] K.A. Willets, P.R. Callis, W.E. Moerner, J. Phys. Chem. B 108 (2004) 10465–10473.
[11] K.A. Willets, O. Ostroverkhova, M. He, R.J. Twieg, W.E. Moerner, J. Am. Chem. Soc. 125 (2003) 1174–1175.
[12] W.E. Moerner, R.J. Tweig, D.W. Kline, M. He, U.S. Patent 20070134737A1, 2007.
[13] H. Kobayashi, M. Ogawa, R. Alford, P.L. Choyke, Y. Urano, Chem. Rev. 110 (2010) 2620–2640.
[14] R.J. Williams, M. Lipowska, G. Patonay, L. Strekowski, Anal. Chem. 65 (1993) 601–605.
[15] M. Berezin, S. Achilefu, Chem. Rev. 110 (2010) 2641–2684.
[16] R.W. Sinkeldam, N.J. Greco, Y. Tor, Chem. Rev. 110 (2010) 2579–2619.
[17] J. Fablan, Chem. Rev. 92 (1992) 1197–1226.
[18] L. Yuan, W. Lin, Y. Yang, H. Chen, J. Am. Chem. Soc. 134 (2012) 1200–1211.
[19] C. Staudinger, S.M. Borisov, Methods Appl. Fluoresc. (2015) 042005.
[20] F. Bures, RSC Adv. 4 (2014) 58826–58851.
[21] G.J. Quinlan, G.S. Martin, T.W. Evans, Hepatology 41 (2005) 1211–1219.
[22] T. Peters, All About Albumin: Biochemistry, Genetics, and Medical Applications, Academic Press Inc., San Diego, USA, 1996.
[23] B.T. Doumas, T. Peters Jr., Clin. Chim. Acta 258 (1997) 3–20.
[24] S. Arques, P. Ambrosi, J. Card. Failure 17 (2011) 451–458.
[25] G. Fanali, A. di Masi, V. Trezza, M. Marino, M. Fasano, P. Ascenzi, Mol. Aspects Med. 33 (2012) 209–290.
[26] M.W. Wu, K. Li, C.Y. Li, J.T. Hou, X.Q. Yu, Chem. Commun. 50 (2014) 183–185.
[27] A. Marini, A. Munoz-Losa, A. Biancardi, B. Mennuci, J. Phys. Chem. B 114 (2010) 17128–17135.
[28] S. Achelle, A. Barsella, C. Baudequin, B. Caro, F. Guen, J. Org. Chem. 77 (2012) 4087–4096.
[29] J. Dashnau, V.N. Nathaniel, K.A.S. Nucci, J.M. Vanderkooi, J. Phys. Chem. B 11 (2006) 13670–13677.
[30] R.B. Singh, S. Mahanta, A. Bagchi, N. Gucchhait, Photochem. Photobiol. Sci. 8 (2009) 101–110.
[31] H.A. Benesi, J.H. Hildebrand, J. Am. Chem. Soc. 71 (1949) 2703–2707.
[32] G.L. Long, J.D. Winefordner, Anal. Chem. 55 (1983) 712–724.
[33] S. Samanta, S. Halder, G. Das, Anal. Chem. 90 (2018) 7561–7568.
[34] S.I. Reja, I.A. Khan, V. Bhalla, M. Kumar, Chem. Commun. 52 (2016) 1182–1185.
[35] T. Gao, S. Yang, X. Cao, J. Dong, N. Zhao, P. Ge, W. Zeng, Z. Cheng, Anal. Chem. 89 (2017) 10085–10093.
[36] X. Fan, Q. He, S. Sun, H. Li, Y. Pei, Y. Xu, Chem. Commun. 52 (2016) 1178–1181.
[37] A.M. Ramezani, J.L. Manzoori, M. Amjadi, A. Jouyban, Sci. World J. 2012 (2012) 1–9.
[38] V. Lhiaubet-Vallet, Z. Sarabia, F. Bosca, M.A. Miranda, J. Am. Chem. Soc. 126 (2004) 9538–9539.
[39] M.C. Jimenez, M.A. Miranda, I. Vaya, J. Am. Chem. Soc. 127 (2005) 10134–10135.
[40] N.E. Basken, C.J. Mathias, M.A. Green, J. Pharm. Sci. 98 (2009) 2170–2179.
[41] I. Petitpas, A.A. Bhattacharya, S. Twine, M. East, S. Curry, J. Biol. Chem. 276 (2001) 22804–22809.
[42] E.S. Krenzel, Z. Chen, J.A. Hamilton, Biochemistry 52 (2013) 1559–1567.
[43] A. Sivertsen, J. Isaksson, H.K.S. Leiros, J. Svenson, J.S. Svendsen, B.O. Brandsdal, BMC Struct. Biol. 14 (2014) 1–14.
[44] A. Nerusu, P.S. Reddy, D.B. Ramachary, R. Subramanyam, ACS Omega 2 (2017) 6514–6524.
[45] M. Fasano, S. Curry, E. Terreno, M. Galliano, G. Fanali, P. Narciso, S. Notari, P. Ascenzi, IUBMB Life 57 (2005) 787–796.
[46] B. Liu, X. Bi, L. McDonald, Y. Pang, D. Liu, C. Pan, Sens. Actuators, Chem. 236 (2016) 668–674.
[47] J. Zhou, G. Lu, H. Wang, J. Zhang, J. Duan, H. Ma, Q. Wu, PLoS ONE 10 (2015) 1–17.
[48] O. Trott, A.J. Olson, J. Comput. Chem. 31 (2009) 455–461.
[49] Z.R. Grabowski, K. Rotkiewicz, Chem. Rev. 103 (2003) 3899–4031.
[50] S. Sasaki, G.P.C. Drummen, G. Konishi, J. Mater. Chem. C 4 (2016) 2731–2743.

Please cite this article in press as: R. Choudhury et al., Tetrahedron Lett. (2018), https://doi.org/10.1016/j.tetlet.2018.06.064